Synthesis, characterization and electrochemical properties of cobalt-doped phosphate tungsten heteropoly acid and its bronze

Jovana S. Ackovic[1], Tamara Petrović[2], Jelena Senćanski[3], Aleksandar Mijatović[4], Stevan Blagojević[3], Pavle Tančić[5], Ružica Micić[1] and Maja Pagnacco[5]

[1]*University of Priština in Kosovska Mitrovica, Faculty of Sciences and Mathematics, Department of Chemistry, Kosovska Mitrovica, Serbia*
[2]*University of Belgrade, Faculty of Physical Chemistry, Belgrade, Serbia*
[3]*University of Belgrade, Institute of General and Physical Chemistry, Belgrade, Serbia*
[4]*University of Belgrade, Faculty of Mining and Geology, Belgrade, Serbia*
[5]*University of Belgrade, Institute of Chemistry, Technology and Metallurgy, Department of Catalysis and Chemical Engineering, Belgrade, Serbia*

Abstract

Heteropoly acids and their compounds are a fascinating class of multifunctional materials for use in various fields: medicine, magnetism, catalysis and nonlinear optics, as well as for electrochemistry and battery materials. This study used tungsten-phosphate heteropoly acid to synthesize and characterize its Co doped salt (Co-PWA) and tungsten-phosphate bronze (Co-PWB). Thermal analysis was used to determine Co-PWA salt phase transition into Co-PWB bronze occurring at 588 °C. Both samples were further characterized using Fourier transform infrared spectroscopy, X-ray powder diffraction and scanning electron microscopy containing energy dispersive X-ray spectroscopy, and by use of electrochemical examinations. Cyclic voltammetry (as a rapid analytical method) showed that both materials yielded low capacities in an aqueous solution of $LiNO_3$. However, a "slow" analytical method, chronopotentiometry, in which more places of a crystal lattice are occupied with ions (as compared to cyclic voltammetry), yielded solid and stable discharge capacity, making Co-PWB attractive as a potential electrode material for aqueous Li-ion batteries. The results obtained fill the gap in the scientific literature dealing with similar materials.

Keywords: Cyclic voltammetry; chronopotentiometry; lithium intercalation/deintercalation reaction; Li-ion batteries

Available on-line at the Journal web address: http://www.ache.org.rs/HI/

ORIGINAL SCIENTIFIC PAPER

UDC: 661.878`027.118:544.6.076.2

Hem. Ind. **79(2)** 103-114 (2025)

1. INTRODUCTION

Heteropoly acids (HPAs) are strong acids composed of heteropoly anions and protons as their counter cations, constituting a special case of heteropoly compounds particularly important for diverse applications [1-4]. Tungsten phosphoric acid (PWA), a special Keggin's type compound, has the general formula $H_3PW_{12}O_{40}\times nH_2O$ ($PWA\times nH_2O$; n = 29, 21, 14, and 6) [5-9]. Tungsten phosphoric salts of heteropoly acids are obtained when one, two, or three acid hydrogen-ions are exchanged with a corresponding number of alkaline, alkaline-earth or other metal ions (cations) [10]. Among other important characteristics of heteropoly acids are that they exhibit very strong Brønsted acidity, act as proton conductors as well as undergo fast, reversible, multi-electron transfers leading to the formation of highly conductive, mixed-valence (*e.g.* tungsten(VI,V) or molybdenum(VI,V), 'heteropoly blue') compounds [9,11]. Heteropoly acids have been applied as electrolytes in electrochemical super capacitors [12]. Phosphate tungsten bronzes (PWBs) have been obtained through PWA thermal treatment [13-15]. These materials exhibit a variety of physical properties, including superconductivity in certain systems [16-17], could be used as electrode materials for Li-ion batteries [18], as well as exhibit interesting electronic and magnetic properties through their incorporation of metal ions into their structure [19]. Due to their 3-dimensional framework, they possess tunnels (*i.e.* channels) in their structure allowing ions such as Li^+, Na^+, K^+ to

Corresponding authors: Jelena Senćanski, Institute of General and Physical Chemistry, University of Belgrade, Studentski trg 12-16, 11000 Belgrade, Serbia
E-mail: jsencanski@iofh.bg.ac.rs
Paper received: 28. September 2024; Paper accepted: 26 May 2025; Paper published: 13 June 2025.
https://doi.org/10.2298/HEMIND240928008A

transport and intercalate within this structure [20,21]. Aside from the structural advantages of PWA and PWB (whose channels allow the intercalation of Li-ions into the structure), high oxidation state of tungsten (W^{6+}) in these compounds prompts their investigation as electrode materials [21,22]. PWA and PWB doped with alkali, earth alkali transition metals, as well as with rare elements have been subject of synthesis and investigation [13,15,16,21-26].

This study deals with novel synthesis and incorporation of Co ions into a heteropoly acid to form Co-PWA salt and its further thermal transformation into Co-PWB bronze. Characterization of these compounds is performed by thermal analysis (*i.e.* thermogravimetric and differential thermal analyses, TGA/DTA), Fourier transform infrared spectroscopy (FTIR), X-ray powder diffraction (XRPD) and scanning electron microscopy using an energy dispersive X-ray spectroscopy (SEM-EDS). Besides the synthesis and characterization of the Co-PWA salt and Co-PWB bronze, which are the main goals of the paper, our second goal was to examine whether these materials might be used as electrode materials for Li-ion batteries. The results obtained could eventually fill the gap in the scientific literature dealing with similar materials.

2. EXPERIMENTAL

2. 1. Synthesis of the studied phases

To carry out the synthesis of heteropoly acid $H_3PW_{12}O_{40}\times29H_2O$, the following procedure was applied: 100 g of $Na_2WO_4\times2H_2O$ (Carl ROTH, Germany) was dissolved in 100 cm^3 of distilled water. Next, 10 cm^3 of 85 % (ρ = 1.70 g cm^{-3}) H_3PO_4 (Merck, Germany) and 80 ml of 37 % (ρ = 1.19 g cm^{-3}) HCl (Merck, Germany) were added. A heteropoly cation is then formed as a white precipitate. Following the solution filtration, the precipitate was transferred to a beaker and dissolved in 100 ml of distilled water, then to a separatory funnel and 70 ml of ether (Carlo Erba, France) and 40 ml of 37 % (ρ = 1.19 g cm^{-3}) HCl were added. The bottom phase presenting the heteropoly acid solution was separated from the other two phases and put into a Petri dish to crystallize (Fig. 1a). Colorless, transparent crystals of $H_3PW_{12}O_{40}\times29H_2O$ (29-PWA; Fig. 1b) were then obtained. These were heated in a kiln at 80 °C to be desiccated for 10 min [13]. After the dehydration of $H_3PW_{12}O_{40}\times29H_2O$ (29-PWA), a compound $H_3PW_{12}O_{40}\times6H_2O$ (6-PWA) was obtained (Fig 1c).

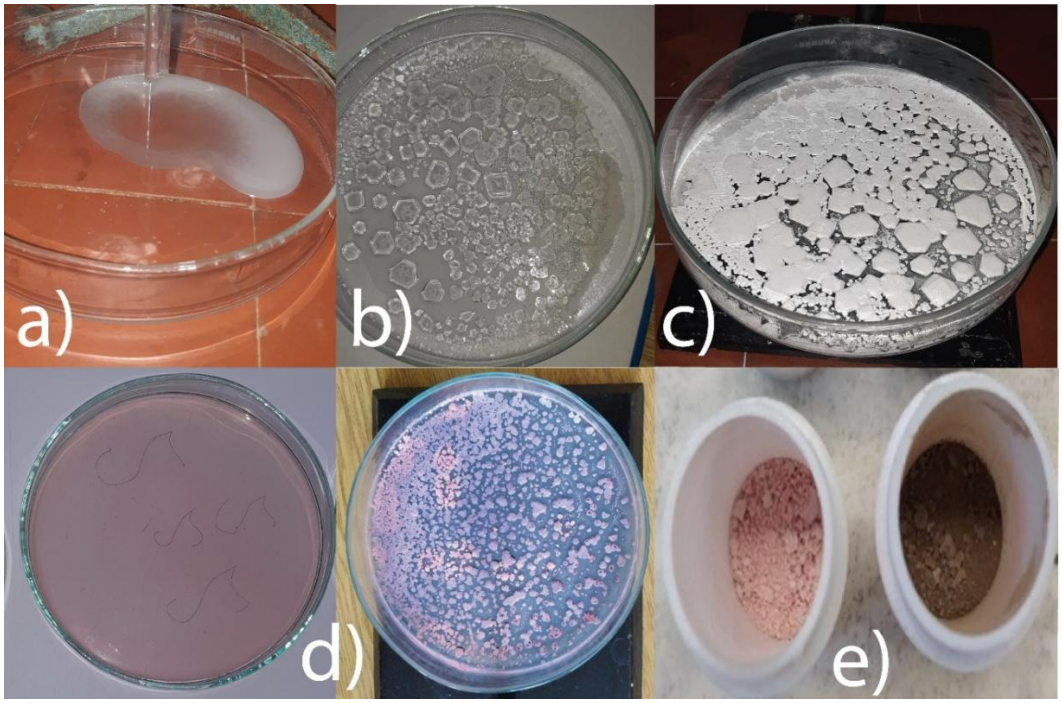

Figure 1. *Presentation of the complete synthesis process: a) heteropoly acid solution; b) beginning of the crystallization; c) formed 6-PWA; d) added $CoCl_2$ salt to the 6-PWA (left- beginning of the crystallization, and right-after crystallization) and e) Co-PWA salt (left) and corresponding Co-PWB bronze (right)*

Ion exchange in equimolar amounts of $CoCl_2\times6H_2O$ resulted in the synthesis of the salts: an aqueous solution of Co-PWA was obtained by dissolving 9.9 g of 6-PWA in distilled water and adding 0.9104 g $CoCl_2\times6H_2O$ in 10 mL of distilled

water. The resulting solution was left overnight at room temperature (~25 °C) to carry out the crystallization process (Fig. 1d; purple-pink). The synthesized Co-PWA is then heated in a furnace at a program starting from room temperature rising to 650 °C (at 10 °C min^{-1}), after which Co-PWB is formed (Fig. 1e right; brown).

2. 2. Thermal examinations

Thermal examinations of Co-PWA were performed using STD 2960 Simultaneous DSC-TGA (TA instruments, USA) using a higher scanning rate (10 °C min^{-1}), rising from room temperature to 900 °C in a nitrogen stream.

2. 3. Fourier-transform infrared spectroscopy

The Co-PWA and Co-PWB samples were characterized by the Fourier-transform infrared spectroscopy (FTIR) method by the instrument PerkinElmer (Thermo Fisher, USA) using the KBr pellet technique with 32 scans and 4 cm^{-1} resolution, at a range of 4000 to 400 cm^{-1}.

2. 4. X-ray powder diffraction

The X-ray powder diffraction (XRPD) patterns of the Co-PWA and Co-PWB phases were obtained using a Rigaku Ultima IV automated diffractometer (Rigaku Corporation, Tokyo, Japan) with a Cu tube operating at 40 kV and 40 mA. The instrument utilizes a curved graphite monochromatic diffraction beam and Xe-filled proportional counter. The diffraction data were collected in the 2θ Bragg angle ranges from 3 to 90°, counting for 2° min^{-1} at every 0.05° steps. The divergence and receiving slits were fixed at 0.5° and 0.15 mm, respectively. The XRPD measurements were performed *ex situ* at room temperature (23 °C) in a stationary sample-holder. The diffractometer alignment was checked by means of a standard Si powder material (Rigaku Corporation, Tokyo, Japan). The Rietveld refinement method and the Fullprof program [27] were further carried out to calculate the unit cell parameters of Co-PWB bronze, according to the procedure described elsewhere [28-30].

2. 5. Scanning electron microscopy - energy dispersive X-ray spectroscopy study

The Co-PWA and Co-PWB samples were first gold-coated, whose morphology, microstructure and chemical composition were studied by scanning electron microscopy (SEM) equipped with an energy dispersive X-ray spectrometer (EDS) using a JEOL 840A instrument (JEOL Ltd., Tokyo, Japan).

2. 6. Electrochemical measurements

Suspensions of the Co-PWA and Co-PWB samples as the active material (85 %), carbon black (10 %; Cabot, Boston, USA) as a conductivity levelling additive, and polyvinylidene fluoride (PVDF; Sigma Aldrich, USA) as the binder (5 %) in the N-methyl-2-pyrrolidone solvent (Carl ROTH, Germany), were used to obtain working electrodes for electrochemical experiments. After being homogenized in an ultrasonic bath, the 10 µl of suspension was pasted on a glassy carbon (GC) electrode, as an electrically conducting support. To evaporate the solvent, the paste was dried for 4 h at 120 °C in a vacuum oven. At room temperature (23 °C), cyclic voltammetry (CV) tests were conducted in a three-electrode cell utilising a Gamry PCI4/300 Potentiostat/Galvanostat (Gamry instruments, Philadelphia, USA). A three-electrode system was used, made of a: (i) working glassy-carbon electrode (GC), (ii) counter electrode (broad-platinum foil) and (iii) saturated-calomel electrode (SCE) (reference electrode). A saturated aqueous solution of $LiNO_3$ (6 M, Carl ROTH, Germany) was used as an electrolyte. The active masses pasted on the glassy-carbon electrodes (working electrodes) of Co-PWA and Co-PWB applied were 1.02 and 0.935 mg, respectively. The masses of cathode materials were determined by multiplying the mass of dried suspensions on electrodes by 0.85.

Chronopotentiometry was carried out by use of three current densities: 1000, 2000 and 3000 mA g^{-1}, in the same three electrode system in the voltage range of -0.9 to 0.7 V *vs.* SCE. The pasted mass on the glassy carbon electrode of the electrode material Co-PWB was 0.00085 g determined as described above. The electrode was manually prepared in the same manner as previously described for cyclic voltammetry.

3. RESULTS AND DISCUSSION

3.1. Thermal characterization

Figure 2 presents the results obtained from the thermogravimetric analysis (TGA), as well as the differential thermal analysis (DTA), *i.e.* the TG and DT curves of $CoHPW_{12}O_{40}\times nH_2O$ (Co-PWA) from room temperature (25 °C) to 900 °C. The DT curve of Co-PWA shows three endothermic peaks at approximately 85, 125 and 185 °C, with an exothermic peak at 588 °C (see Fig. 2). The three endothermic peaks found in the DT curve of Co-PWA at low temperatures may be attributable to the physisorbed (up to ~100 °C) and crystal (up to ~450 °C) water liberation [31]. The H_2O content within the Co-PWA salt was estimated from the total TG weight loss of ~8.39 wt.% between room temperature and ~450 °C. Such weight loss corresponds to the calculated water content of *ca.* 15 moles of H_2O in the salt structure, which agrees with the $CoHPW_{12}O_{40}\times 15H_2O$ composition. Further, the solid-solid structural phase transformation from the anhydrous heteropoly Co-PWA salt to the Co-doped phosphate tungsten bronze was determined through the exothermic reaction, which occurred at 588 °C.

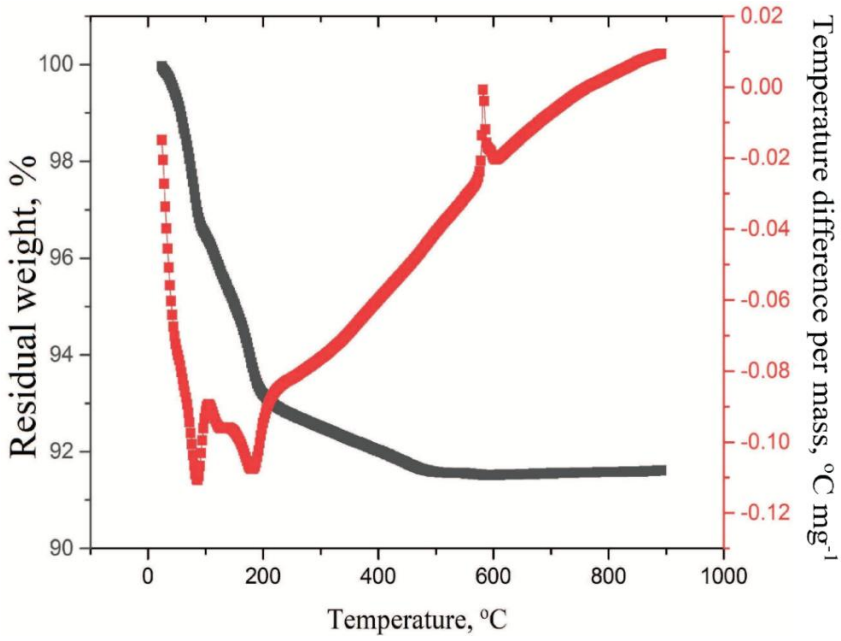

Figure 2. TGA (full line) and DTA (dashed line) curves of $CoHPW_{12}O_{40}\times nH_2O$

3. 2. Structural characterization

3. 2. 1. Comparison of cobalt tungsten doped salt and cobalt tungsten-phosphate bronze

FTIR spectra of the Co-PWA salt and Co-PWB bronze are presented in Figure 3. Table 1 presents assigning of FTIR bands for Co-PWA salt and Co-PWB bronze.

***Table 1**. The characteristic FTIR bands of Co-PWA and Co-PWB*

Co-PWA		Reference	Co-PWB		Reference
Wavenumber, cm^{-1}	Assignation		Wavenumber, cm^{-1}	Assignation	
3457 vs	v_3 (H_2O)	[32]	1118 m	v_3 (PO_4)	[21]
1732 sh	v_4 (H_3O^+)	[32,33]	904 sh	v (W-O-W)	[32,34]
1616 m	v_2 (H_2O)	[32]	766 vs	v (W-O-W)	[34]
1075 s	v_3 (PO_4)	[13,32,34]	~400	v_4 (PO_4)	[32]
976 s	v_1 (PO_4)	[13]			
893 m	v (W-O-W)	[32,34]			
797 s	v (W-O-W)	[34]			
594 w	v_4 (PO_4)	[13]			

Marks: vs-very strong, s-strong, m-medium, w-weak, sh-shoulder, v characteristic vibrations of WO_6 octahedron, v_1-symmetric stretching, v_2 bending, v_3-antisymmetric stretching, v_4-bending

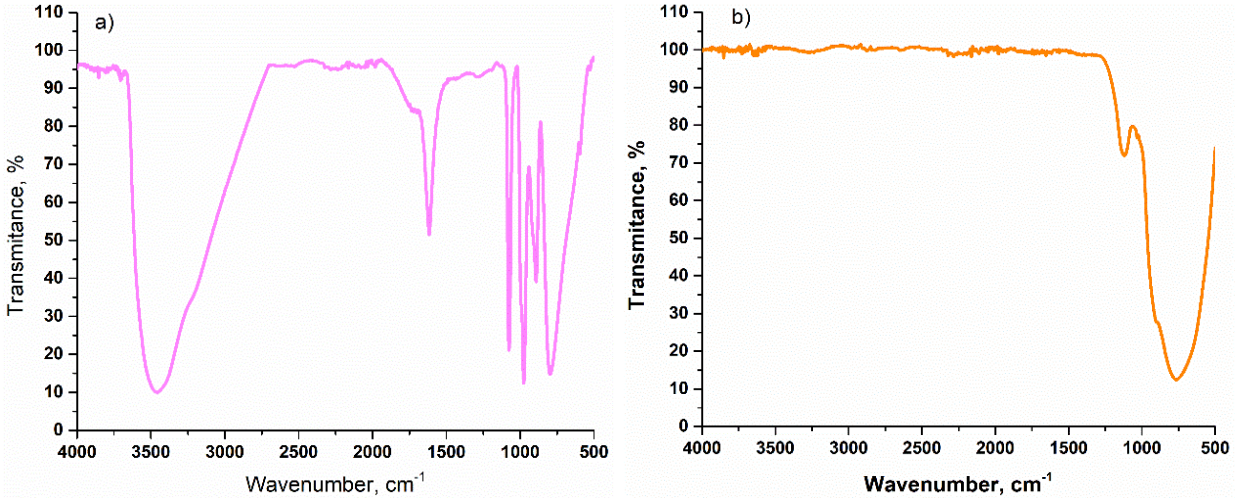

Figure 3. *FTIR spectra of: a) Co-PWA and b) Co-PWB*

The FTIR spectrum of cobalt-doped heteropoly salt, Co-PWA, shows characteristic vibrational modes associated with the Keggin structure [13], which contain displacements or changes in intensity due to cobalt doping. Characteristic bands for the H_2O molecule are found at wavenumbers in the Co-PWA infra-red spectrum (Table 1): v_1 = 3457 cm^{-1} and v_2 = 1616 cm^{-1} [32]. The shoulder present in the higher wavenumber region (~1732 cm^{-1}) of the bands corresponding to the bending vibration of H_3O^+ ion [32] was also evident in Fe-PWA [21]. Typical vibrations of PO_4 tetrahedra are bands placed at wavenumbers in the Co-PWA spectrum: v_3 = 1075 cm^{-1} [13,32,34], v_1 = 976 cm^{-1} [13] and v_4 = 594 cm^{-1} [13]; while the bands characteristic for vibration of the WO_6 octahedron are located at wavenumbers in the Co-PWA spectrum: v = 893 cm^{-1} [32,34] and v = 797 cm^{-1} [34]. The characteristic vibrational modes of the PO_4 tetrahedron and WO_6 octahedron were reported to be positioned at similar wavenumbers in the FTIR spectra for PWA [13].

After the thermal treatment of the Co-PWA salt, the FTIR spectrum displayed evident changes obviously due to the Co-PWB formation. The phase transformation related to the collapse of the Keggin's structure (*i.e.* complete liberation of water molecules and rearrangement of PO_4 and WO_6 units) and formation of Co-PWB bronze are shown in Figure 3b and Table 1. The band positioned at v_3 = 1118 cm^{-1} in the Co-PWB spectrum is associated with the characteristic vibration of PO_4 tetrahedron [21]; while the shoulder at v = 904 cm^{-1}, and a very strong band at v = 766 cm^{-1} are associated with characteristic vibrations of WO_6 octahedron [34]. The band positioned at ~400 cm^{-1} corresponds to the characteristic vibration of the PO_4 unit [32]. A comparable spectrum was also obtained for another reported bronze Fe-PWB [21].

3. 2. 2. XRPD characterization

XRPD patterns of Co-PWA and Co-PWB phases are presented at Figure 4 and Table 2, while the calculated unit-cell parameters are shown in Table 3.

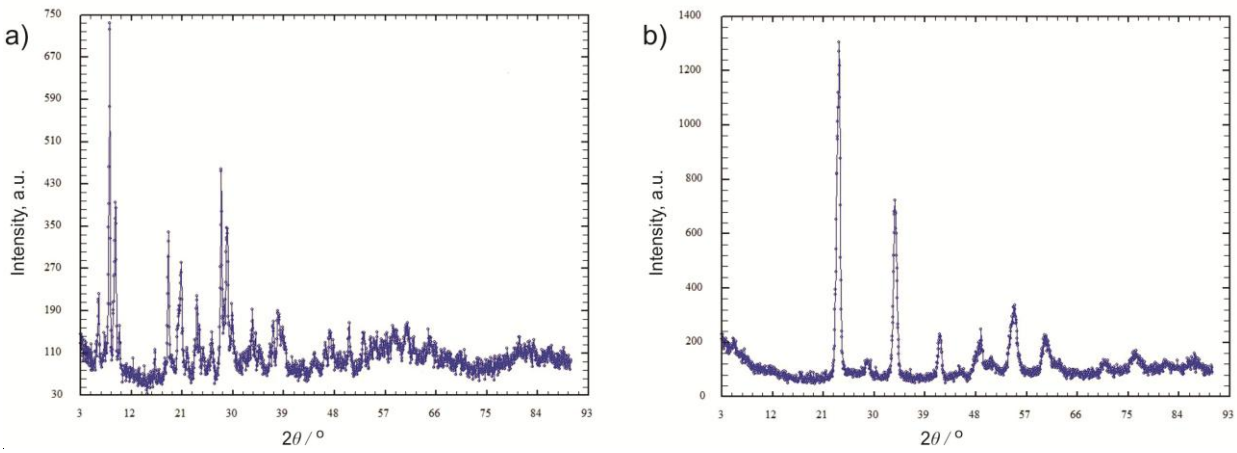

Figure 4. *XRPD patterns determined for: a) Co-PWA; and b) Co-PWB*

Table 2. *Determined interplanar spacings (d_{det}), and intensities (I_{det}) of the Co-PWA and Co-PWB phases (note: data for monoclinic PWB [13] are also presented for comparison).*

Co-PWA		Co-PWB		monoclinic PWB		
d_{det} / nm*	I_{det} / %	d_{det} / nm*	I_{det} / %	d_{det} / nm	I_{det} / %	hkl
1.433(8)	18	/	/	0.384	41	0 0 2
1.078(1)	100	0.3738(2)	100	0.375	100	0 2 0
0.9531(6)	49	0.3107(4)	4	0.311	6	-1 1 2
0.890(4)	10	0.2660(1)	54	0.268	40	-2 0 2
0.4775(6)	44	/	/	0.264	26	2 0 2
0.4254(3)	29	0.2170(2)	14	0.217	14	-2 2 2
/	/	/	/	0.201	2	2 1 3
0.3771(6)	20	/	/	0.192	3	0 0 4
0.3191(2)	56	0.1866(3)	8	0.187	11	-1 0 4
0.3071(2)	38	0.1798(7)	2	0.181	4	-1 1 4
0.2985(6)	12	0.1678(1)	18	0.167	15	-2 1 4
0.2676(6)	6	0.1533(2)	10	0.153	9	2 4 2
0.234(1)	10	/	/	0.149	3	-1 4 3
/	/	0.12478(9)	4	/	/	/

*The numbers in parentheses are the estimated standard deviations and refer to the last significant number

Table 3. *Calculated unit cell parameters of Co-PWB compared to the reported values for PWB [13]*

	Co-PWB*	PWB*
a_0 / nm	0.745(2)	0.7325(6)
b_0 / nm	0.744(2)	0.7516(9)
c_0 / nm	0.759(1)	0.7686(9)
β_0 / °	89.5(2)	90.79(5)
V_0 / nm^3	0.421(2)	0.4231(9)

*The numbers in parentheses are the estimated standard deviations and refer to the last significant number

Concurring with our previous results [13,21], these two phases are disparate, confirming the solid-solid structural phase transformation observed by the thermal analysis (Fig. 2) and FTIR results (Fig. 3 and Table 1). According to the herein obtained data and bronze data reported elsewhere [13,21,24,25], it could be reasonably assumed that all these compounds are iso-structural, *i.e.* that Co-PWB crystallized in the monoclinic crystallographic system.

Table 3 presents the calculated Co-PWB unit-cell parameters including those reported for un-doped PWB bronze. From these results, it is obvious that the entrance of Co ions into the PWB structure resulted in an increase in the a_0 axis, while all the other parameters were decreased (*i.e.* axes b_0 and c_0, angle β_0 and volume V_0). Co-PWB has almost mutually identical a_0 and b_0 axes (similarly to the Fe-PWB [21]); however, the significant deviation of the angle β_0 from 90° excludes in this case the possibility for its crystallization in a tetragonal crystallographic system.

3. 3. Morphological characterization

Figures 5a and 5c present morphology of the materials Co-PWA salt and Co-PWB bronze. Cracks in the agglomerated plates for both compounds are most probably the consequence of the synthesis procedure by which water evaporates.

To detect chemical elements, EDS line scans were carried out for both samples, as presented in Figures 5b and 5d. The chemical elements: O, W, Co and P were detected in both, where differing atomic and weight concentrations of W, O, P and Co were observed. The reason for such behavior most probably might lie in the inhomogeneous distribution of the particles in the samples studied. Nevertheless, these results confirm the entering of Co into the both PWA and PWB compounds, which is in line with the above-discussed FTIR and XRPD studies.

3. 4. Electrochemical characterization

3. 4. 1 Cyclic voltammetry measurements

Often used as a rapid analytical method, cyclic voltammograms (CVs) were obtained at a scan rate of 20 mV s^{-1} for all samples measured within their potential corresponding electrochemical stability windows (+0.09 to -0.85 V *vs.* SCE for Co-PWA; Fig. 6a; and +0.6 to -1.0 V vs. SCE for Co-PWB; Figs. 6b,c), and a 5 mV s^{-1} was also applied for Co-PWB (Fig. 6d).

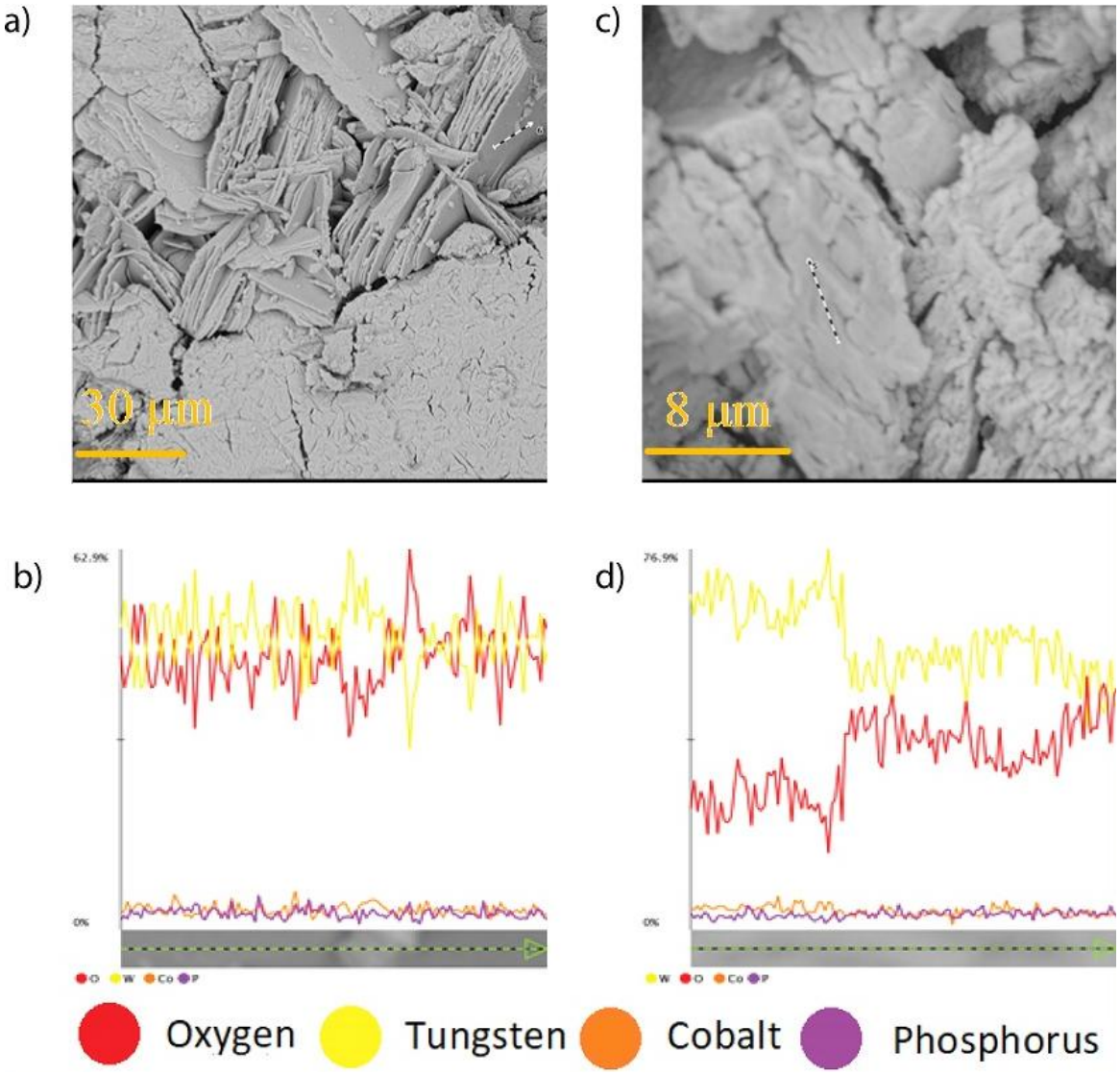

Figure 5. *SEM-EDS scanning: a) SEM presenting the entire region and a line scan (marked in black and white arrows) of Co-PWA; b) the combined EDS line scan of Co-PWA; c) SEM presenting the entire region and a line scan (marked in black and white arrows) of Co-PWB; d) the combined EDS line scan of Co-PWB. The Y axes correspond to atomic mass percents, while the X axes are mapping lines presented in Figures 5a) and 5c). For interpretation of the references to colour in this figure legend, the reader is referred to the web version of this article*

The Co-PWA CV (reduction during the 1st cycle) is composed of four ion insertion peaks at -0.2, -0.39, -0.56 and -0.74 V *vs.* SCE (Fig. 6a). A tentative explanation is that Li^+ ions entered the Co-PWA, thereby causing a formation of four distinct phases of $CoLi_x$-PWA salt. The first de-insertion process for Co-PWA was followed by anodic peaks positioned at -0.67 and -0.14 V *vs.* SCE. Deposition of the material over the ions insertion caused a significant distinction between the cathodic and anodic capacity. The formed unstable electrode material precipitated in an aqueous solution of $LiNO_3$ (see Supplementary Material, Fig. S1.) resulting in a low anode capacity, due to which there was not sufficient electrode material remaining on the glassy carbon electrode for the ions' de-insertion. As proven by the immersion of the electrode in an aqueous solution of $LiNO_3$, Co-PWA was not displaced from the working electrode into the electrolyte prior to the ions insertion (Supplementary Material, Fig. S1.). The insertion of ions, therefore, probably leads to the formation of $CoLi_x$-PWA salt unstable in the electrolyte. As previously determined, Fe-PWA exhibited the same behavior over the first cathode cycle in the same electrolyte [21]. Based on the results obtained, while demonstrating that the Co-PWA salt is not usable as an electrode material for aqueous Li-ion batteries, its redox activity deserves further examination in other electrolytes, especially in non-aqueous ones.

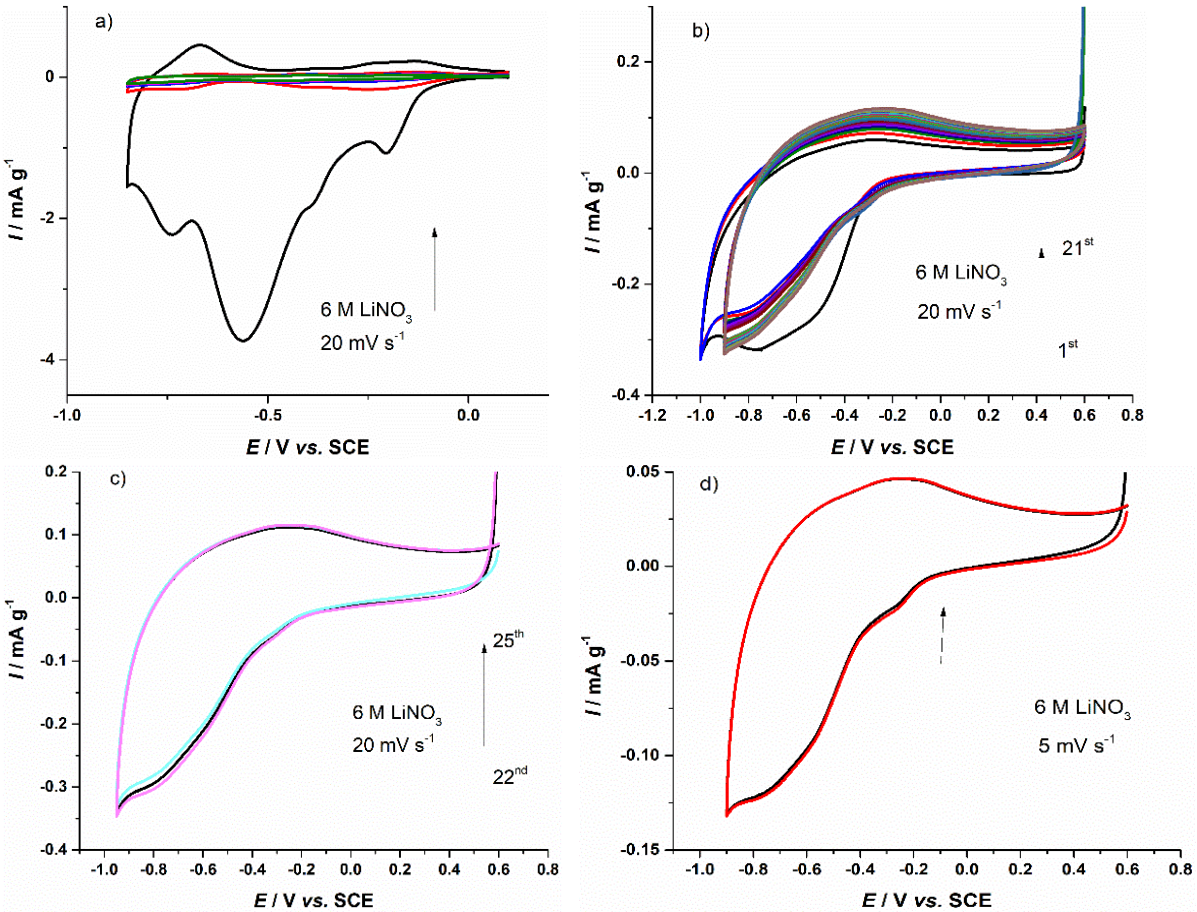

Figure 6. *Cyclic voltammetry measurements: a) CVs of Co-PWA; b) CVs of Co-PWB recorded at 20 mV s^{-1} 1st to 21st cycle; c) CVs of Co-PWB recorded at 20 mV s^{-1} 22nd to 25th cycle ; and d) CV obtained at a scanning rate of 5 mV s^{-1} for Co-PWB*

Compared to the four clearly visible peaks for ions insertion in Co-PWA, the structure of its corresponding bronze Co-PWB allows only two small and broad peaks (*i.e.* -0.26 and -0.74 V *vs.* SCE) when polarization rate was 5 mV s^{-1} (Fig. 6d), which are not visible at a higher polarization rate of 20 mV s^{-1} (Figs. 6b and 6c). The initial enhanced electrochemical activity of the Co-PWA salt compared to its thermally obtained bronze is likely a consequence primarily of: (i) different structures between the Co-PWA and Co-PWB compounds; and (ii) the presence of water in the Co-PWA structure, which is lacking in the Co-PWB structure, as unquestionably determined in the present studies (see Figs. 3 and 4; and Tables 1 and 2). Such a situation in Co-PWA obviously provides additional sites for ion-intercalation [31]. However, the potential intercalation of ions into Co-PWA makes it far less stable compared to its corresponding bronze Co-PWB. On the other hand, the stability of Co-PWB was achieved after 21st cycle, as observed in Figs. 6b and 6c. A higher cathode capacity compared to the anodic one for Co-PWB means that the insertion of ions is a more favorable process compared to de-insertion.

When doped, PWB metallic behavior becomes corrupted due to electrons filling the W-O-W hybridized π* conduction band [35-37] changing the metallic behavior of PWB from a semiconductor to an insulator. Consequently, all doped samples exhibit decreased electrical conductivity compared to the un-doped PWB sample. The lithium-doped bronzes (Li_3-PWB and Li_n-PWB) exhibit both: (i) sluggish kinetics of broad and barely visible peaks, as well as (ii) irreversible delithiation caused by structural transformation [26]. Similar forms of the CVs is noted for Fe-PWB [21], Co-PWB [this work], and Li_3-PWB [26]. Compared to Li^+ in Li_3-PWB, doping with more charged ions (*e.g.* Co^{2+} and Fe^{3+}), therefore, seemingly protects the bronze structure from transformation into its unstable form in $LiNO_3$ aqueous solution caused by ion insertion.

3. 4. 2. Chronopotentiometry measurements of cobalt tungsten-phosphate bronze

To simulate the charge and discharge of the electrode material as if in a battery, the chronopotentiometry method was applied for Co-PWB in a 6M aqueous solution of $LiNO_3$. The three rates of 1000, 2000 and 3000 mA g^{-1} were applied to

charge and discharge the electrode material. The charge and discharge curves are presented in Figure 7a, while dependences of discharge capacities on the cycle number obtained for each current are presented in Figure 7b.

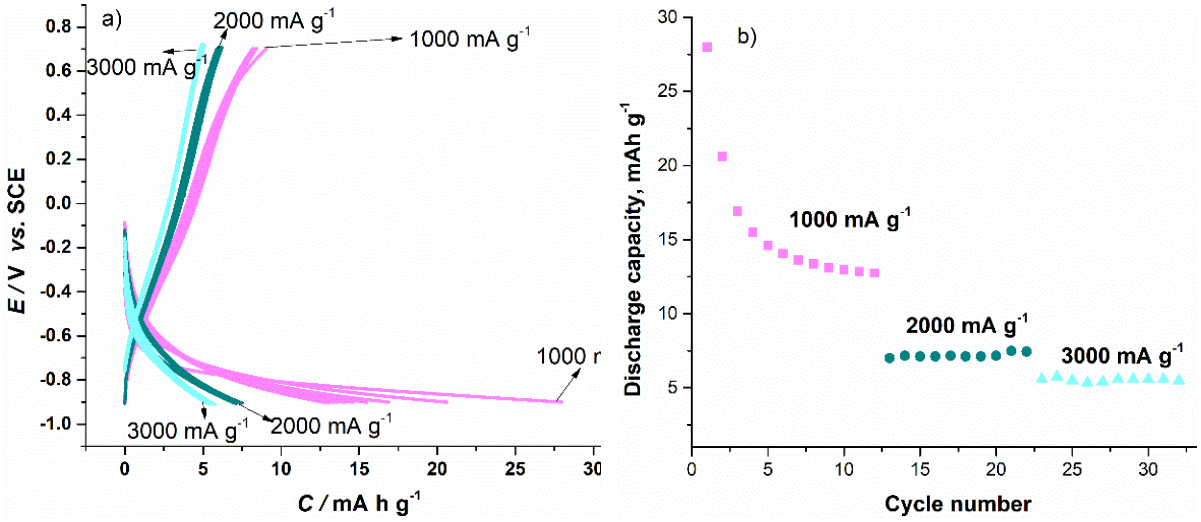

***Figure 7**. Chronopotentiometry measurements: a) charging and discharging cycles of Co-PWB; and b) discharge capacity vs. cycle number of Co-PWB in an aqueous solution of 6 M $LiNO_3$*

According to the herein obtained results, the initial capacity for 1000 mA g^{-1} was ~28 mAh g^{-1}, while stabilization was achieved after the tenth cycle yielding a capacity of ~13 mAh g^{-1}. Compared to a reported study [26] in which the material PWB was examined, the initial capacity obtained was ~67 mAh g^{-1} and after stabilization reached ~25 mAh g^{-1} at a polarization rate of 100 mA g^{-1}; the results obtained indicate that the material Co-PWB has a potential for higher capacities at slower currents applied. In the present study, the capacity was stabilized just after the tenth cycle, although the literature [26] indicates that capacity stabilization may be achieved after one hundred cycles. Further, stabilization of the material was accomplished immediately when the currents applied were 2000 and 3000 mA g^{-1}, indicating that a stable structure was achieved over the charging and discharging processes under the application of such higher current rates. Therefore, chronopotentiometry showed that Co-PWB has a potential as an electrode material for aqueous Li-ion batteries.

4. CONCLUSION

This research has aimed to synthesize novel heteropoly materials Co-PWA salt and its bronze Co-PWB obtained by the thermal treatment of Co-PWA at an intermediate temperature (588 °C). The materials were characterized using XRPD, FTIR, SEM, EDS, cyclic voltammetry, as well as chronopotentiometry methods. The presence of Co was undoubtedly confirmed in both Co-PWA salt and Co-PWB bronze, thereby verifying their successful syntheses. Both cyclic voltammetry and chronopotentiometry yielded stable capacities. Based on the results obtained, Co-PWB might be a promising electrode material. The results obtained bridge the gap in the scientific literature on these and similar materials.

SUPPLEMENTARY MATERIAL

Additional data are available electronically at https://www.ache-pub.org.rs/index.php/HemInd/article/view/1384, or from the corresponding author on request.

Acknowledgement: *This work was financially supported by the Ministry of Science, Technological Development and Innovation of the Republic of Serbia (Grants No. 451-03-66/2024-03/200026, 451-03-66/2024-03/200051, 451-03-66/2024-03/200146 and 451-03-65/2024-03/200126) and the Faculty of Science and Mathematics, University of Priština in Kosovska Mitrovica (Grant No. IJ-2301). The authors thank Dr Zoran Nedić for his useful help in preparing the materials in the bronze synthesis. M.P. acknowledges the support of the EU: the EIC Pathfinder Challenges 2022 call through the Research Grant 101115149 (project ARTEMIS), as well as the support of the Office of Naval Research Global through the Research Grant N62902-22-1-2024.*

REFERENCES

[1] Kamiya Y, Okuhara T, Misono M, Miyaji A, Tsuji K, Nakajo T. Catalytic chemistry of supported heteropolyacids and their applications as solid acids to industrial processes. *Catal Surv Asia.* 2008; 12: 101-113. https://doi.org/10.1007/s10563-008-9043-7

[2] Chikin AI, Chernyak AV, Jin Z, Naumova YS, Ukshe AE, Smirnova NV, Volkov VI, Dobrovolsky YA. Mobility of protons in 12-phosphotungstic acid and its acid and neutral salts. *J Solid State Electrochem.* 2012; 16: 2767-2775. https://doi.org/10.1007/s10008-012-1687-6

[3] Kourasi AM, Wills RGA, Shah AA, Walsh FC. Heteropolyacids for fouel cell applications. *Electrochim Acta.* 2014; 127: 454-466. https://doi.org/10.1016/j.electacta.2014.02.006

[4] Imofeeva MN, Maksimov GM, Likholobov VA. Acidity of solutions of heteropoly acids with various structures and compositions. *Kinetic Catal.* 2001; 42: 30-34. https://doi.org/10.1023/A:1004892411282

[5] Kima JD, Hayashi S, Mori T, Honma I. Fast proton conductor under anhydrous condition synthesized from 12-phosphotungstic acid and ionic liquid. *Electrochim Acta.* 2007; 53: 963-967. https://doi.org/10.1016/j.electacta.2007.08.009

[6] Schneea J, Devredb F, Gaigneauxb EM, Vimonta A, Assessing the dispersion of supported $H_3PW_{12}O_{40}$ catalysts: No longer a hurdle thanks to in situ IR upon pyridine adsorption. *Appl Catal.* 2019; 578: 116-121. https://doi.org/10.1016/j.apcata.2019.03.022

[7] Brown GM, Noe-Spirlet MR, Busing WR, Levy HA. Dodecatungstophosphoric acid hexahydrate, $(H_5O_2^+)_3(PW_{12}O_{40}^{3-})$. The true structure og Keggins pentahydrate from single-crystal X-ray and neutron diffraction data. *Acta Cryst.* 1977; B33: 1038-1046. https://doi.org/10.1107/S0567740877005330

[8] Spirlet MR, Busing WR. Dodecatungstophosphoric acid-21-water by neutron diffraction. *Acta Cryst.* 1978; 34(3): 907-910. https://doi.org/10.1107/S0567740878004306

[9] Kremenović A, Spasojević-de Biré A, Dimitrijević R, Sciau P., Mioč UB, Colomban Ph. Keggin's ion structural modification and expansion of dodecatungstophosphoric acid hexahydrate induced by temperature treatment: In situ X-ray powder diffraction and Raman investigations. *Solid State Ion.* 2000; 132: 39-53. https://doi.org/10.1016/S0167-2738(00)00727-X

[10] Davidović M, Čajkovski T, Colomban Ph, Mioč UB, Likar-Smiljanić V, Čajkovski D, Biljić R, Nedić Z. The influence of monovalent and bivalent cations on the electrical properties of 12-tungstophosphoric acid salts. *Solid State Ion.* 2005; 176: 2881-2885. https://doi.org/10.1016/j.ssi.2005.09.020

[11] Kulesza PJ, Rutkowska IA, Janiszewska C, Noto VD, Vezzu K, Negro E. Development and characterization of polyoxometallate-based systems for aqueous redox flow batteries. *Meet Abstr.* 2022; MA2022-01: 1999. https://doi.org/10.1149/MA2022-01481999mtgabs

[12] Ammam M, Fransaer J. Ionic liquid-heteropolyacid: Synthesis, characterization, and supercapacitor study of films deposited by electrophoresis. *J Electrochem Soc.* 2011; 158: A14. https://doi.org/10.1149/1.3507254

[13] Mioč UB, Dimitrijević RŽ, Davidović M, Nedić ZP, Mitrović MM, Colomban Ph. Thermally inducted phase transformations of 12-tungstophosphoric acid 29-hydrate:synthesis and characterization of PW_8O_{26}-type bronzes. *J Mater Sci.* 1994; 29: 3705-3718. https://doi.org/10.1007/BF00357338

[14] Dimitrijević RŽ, Colomban Ph, Mioč UB, Nedić Z, Todorović MR, Tjapkin N, Davidović M. Synthesis, conductivity and structural characterization of phosphorous bronzes originating from heteropolyacids. Relation with similar proton containing phases. *Solid State Ion.* 1995; 77: 250-256. https://doi.org/10.1016/0167-2738(94)00310-O

[15] Maksimović TV, Maksimović JP, Joksović LjG, Nedić ZP, Pagnacco MC. Oscilatorna reakcija kao sistem detektor za dopirane i nedopirane fosfat-volframove bronze. *Hem Ind.* 2018; 72(5): 275-283. (in Serbian) https://doi.org/10.2298/HEMIND180402018M

[16] Sweedler AR, Raub ChJ, Matthias BT. Superconductivity of the alkali tungsten bronzes. *Phys Lett.* 1965; 15(2): 108-109. https://doi.org/10.1016/0031-9163(65)91292-8

[17] Brusetti R, Bordet P, Bossy J, Schober H, Eibl S. Superconductivity in the tungsten bronze Rb_xWO_3 ($0.20 \leqslant x \leqslant 0.33$) in connection with its structure, electronic density of states, and phonon density of states. *Phys Rev.* 2007; B76: 174511. https://doi.org/10.1103/PhysRevB.76.174511

[18] Yoon S, Jo C, Noh SY, Lee CW, Song H, Lee J. Development of a high-performance anode for lithium ion batteries using novel ordered mesoporous tungsten oxide materials with high electrical conductivity. *PCCP.* 2011; 13: 11060-11066. https://doi.org/10.1039/C1CP20940J

[19] Wasserman K, Pope MT, Salmen M, Dann JN, Lunk HJ. Thermal degradation of polyoxotungstates-an effective method for the preparation of tungsten bronzes. *J Solid State Chem.* 2000; 149: 378-383. https://doi.org/10.1006/jssc.1999.8556

[20] Dong X, Lu Y, Wu Z, Liu X, Tong Y. Photochromic hierarchical $(NH_4)_xWO_3$ nanocrystals with bronze tunnel structure for energy-saving windows. *Chem Eng J.* 2023; 477: 147064. https://doi.org/10.1016/j.cej.2023.147064

[21] Acković J, Micić R, Nedić Z, Petrović T, Senćanski J, Pagnacco M, Tančić P. Synthesis, characterization and electrochemical properties of iron doped phosphate tungsten heteropoly acid (Fe-PWA) and its bronze (Fe-PWB): Comparative study. *Sci Sinter.* 2024; 56: 367-380. https://doi.org/10.2298/SOS230812053A

[22] Pagnacco M, Marković S, Potočnik J, Krstić V, Tančić P, Mojović M, Mojović Z. The influence of electrode constituents on hydrogen evolution reaction on phosphate W-and Mo bronze based electrodes. *J Electrochem Soc.* 2022; 169(10): 106508. https://doi.org/10.1149/1945-7111/ac96ab

[23] Maksimović JP, Maksimović TV, Nedić ZP, Pagnacco MC. The minor influence of calcium doped phosphate tungsten bronze on the Briggs-Rauscher reaction dynamics. *Contemp Mater.* 2018; 184-189. https://doi.org/10.7251/COMEN1802184M

[24] Maksimović TV, Maksimović JP, Tančić PI, Potkonjak NI, Nedić ZP, Joksović LjG, Pagnacco MC. A possible connection between phosphate tungsten bronzes properties and Briggs-Rauscher oscillatory reaction response. *Sci Sinter.* 2021; 53: 223. https://doi.org/10.2298/SOS2102223M

[25] Maksimović T, Tančić P, Maksimović J, Mara D, Ilić M, Van Deun R, Joksović Lj, Pagnacco M. Novel cerium and praseodymium doped phosphate tungsten bronzes: Synthesis, characterization, the behavior in the Briggs-Rauscher reaction and photoluminescence properties. *Opt Mater.* 2023; 143: 114125. https://doi.org/10.1016/j.optmat.2023.114125

[26] Vujković M, Nedić Z, Tančić P, Aleksić OS, Nikolić MV, Mioč U, Mentus S. Electrochemical lithiation/delithiation kinetics and capacity of phosphate tungsten bronze and its chemically pre-lithiated derivatives aqueous solutions. *J Mater Sci.* 2016; 51: 2481-2489. https://doi.org/10.1007/s10853-015-9560-5

[27] Rodriguez-Carvajal, J. Program Fullprof (Computer software). In Proceedings of the Abstract of 15th Conference of International Union of Crystallography, Satellite Meeting on Powder Diffraction, Toulouse, France, July 16-19th 1990; p. 127.

[28] Tančić P, Dimitrijević R, Poznanović M, Pačevski A, Sudar S. Crystal structure and chemical composition of ludwigite from Vranovac ore deposit (Boranja Mountain, Serbia). *Acta Geol Sin-Engl.* 2012; 86(6): 1524-1538. https://doi.org/10.1111/1755-6724.12020

[29] Tančić P, Kremenović A, Vulić P. Structural dissymmetrization of optically anisotropic $Grs_{64\pm1}Adr_{36\pm1}Sps_2$ grandite from Meka Presedla (Kopaonik Mt., Serbia). *Powder Diffr.* 2020; 35(1): 7-16. https://doi.org/10.1017/S0885715619000897

[30] Tančić P, Kremenović A. Rietveld crystal structure refinement of a natural rhombohedral grossular-andradite garnet from Serbia. *Geol Q.* 2022; 66(7): 1639. http://dx.doi.org/10.7306/gq.1639

[31] Mioč U, Davidović M, Tjapkin N, Colomban Ph, Novak A. Equilibrium of the protonic species in hydrates of some heteropolyacids at elevated temperatures. *Solid State Ion.* 1991; 46: 103-109. https://doi.org/10.1016/0167-2738(91)90136-Y

[32] Ratajczak H, Barnes AJ, Bielański A, Lutz HD, Müller A, Pope MT. Vibrational Spectroscopy of Heteropoly Acids. In: Pope, MT, Müller A. (eds) Polyoxometalate Chemistry From Topology via Self-Assembly to Applications. *Springer Dordrecht*. 2001; 101-116. https://doi.org/10.1007/0-306-47625-8_8

[33] Jose da Silva M, Macedo de Oliveira C. Catalysis by Keggin heteropolyacid salts. *Curr Catal.* 2018; 7: 26-34. https://doi.org/10.2174/2211544707666171219161414

[34] Rocchiccioli-Deltcheff C, Fournier M, Franck R, Thouvenot R, Vibrational investigations of polyoxometalates. 2. Evidence for anion-anion interactions in molybdenum(VI) and tungsten(VI) compounds related to the keggin structure. *Inorg Chem.* 1983; 22: 207-216. https://doi.org/10.1021/ic00144a006

[35] Martinez-de la Cruz A, Rodriguez FEL, Rodriguez JI. Electrochemical lithium insertion in the phosphate tungsten bronze $P_8W_{12}O_{52}$. *Solid State Ion.* 2005; 176: 2625-2630. https://doi.org/10.1016/j.ssi.2005.08.009

[36] Martínez-de la Cruz A, Rodríguez FEL. Electrochemical lithium insertion in $(PO_2)_4(WO_3)_{2m}$ ($2 \leq m \leq 10$): Relation among the electrochemical insertion process and structural features. *Electrochim Acta.* 2009; 54: 3176-3183. https://doi.org/10.1016/j.electacta.2008.11.056

[37] Wang E, Greenblatt M. Lithium and sodium insertion reactions of phosphate tungsten bronzes. *J Solid State Chem.* 1987; 68: 38-44. https://doi.org/10.1016/0022-4596(87)90282-9

Sinteza, karakterizacija i elektrohemijske osobine kobaltom dopirane fosfat volframove heteropoli kiseline i njene bronze

Jovana S. Ackovic[1], Tamara Petrović[2], Jelena Senćanski[3*], Aleksandar Mijatović[4], Stevan Blagojević[3], Pavle Tančić[5], Ružica Micić[1] i Maja Pagnacco[5]

[1]*Univerzitet u Prištini, Prirodno-matematički fakultet, Departman za hemiju, Kosovska Mitrovica, Srbija.*
[2]*Univerzitet u Beogradu, Fakultet za fizičku hemiju, Beograd, Srbija.*
[3]*Univerzitet u Beogradu, Institut za opštu i fizičku hemiju, Beograd, Srbija.*
[4]*Univerzitet u Beogradu, Rudarsko-geološki fakultet, Beograd, Srbija.*
[5]*Univerzitet u Beogradu, Institut za hemiju, tehnologiju i metalurgiju, Katedra za katalizu i hemijsko inženjerstvo, Beograd, Srbija*

(Naučni rad)

Izvod

Heteropoli kiseline i njihova jedinjenja su fascinantna klasa multifunkcionalnih materijala koji se koriste u različitim naučnim oblastima: medicini, magnetizmu, katalizi, nelinearnoj optici kao i u elektrohemiji gde se primenjuju kao materijali za baterije. U ovoj studiji je polazna tačka volfram-fosfatna heteropoli kiselina iz koje je sintetisana i karakterisana njena kobaltova so (Co-PWA) i kobaltom dopirana volfram-fosfatna bronza (Co-PWB). Termička analiza je korišćena za određivanje faznog prelaza Co-PWA soli u Co-PWB bronzu koji se odvija na 588 °C. Ova temperatura je korišćena za žarenje Co-PWA da bi se sintetisala Co-PWB. Oba uzorka su dalje karakterisana korišćenjem infracrvene spektroskopije sa Furijeovom transformacijom (engl. Fourier transform infrared spectroscopy), difrakcije rendgenskih zraka na prahu (engl. X-ray powder diffraction) i skenirajuće elektronske mikroskopije koja sadrži energetsku disperzivnu rendgensku spektroskopiju (engl. scanning electron microscopy using an energy dispersive X-ray spectroscopy), kao i korišćenjem elektrohemijskih ispitivanja. Prisustvo kobalta je nedvosmisleno pokazano i u Co-PWA i Co-PWB, pri cemu je potvrdjeno uspešno dopiranje. Za elektrohemijska ispitivanja korišćene su ciklična voltametrija kao "brza" tehnika i metoda hronopotenciometrije radi simuliranja punjenja i pražnjenja baterije. Ciklična voltametrija je izmerila nestabilan i mali kapacitet za Co-PWA i stabilan za Co-PWB u vodenom rastvoru $LiNO_3$. Razlog pada kapaciteta kod Co-PWA je nestabilnost ove soli u navedenom elektrolitu. Zbog stabilnog kapaciteta Co-PWB dobijenim merenjem cikličnom voltametrijom, ovaj material je podvrgnut hronopotenciometrijskom punjenju i pražnjenju pri strujama 1000, 2000 i 3000 mA g^{-1}. Ovom metodom je pokazan stabilan kapacitet pri svakoj od primenjenih struja, što ga čini atraktivnim elektrodnim materijalom za vodene Li-jonske baterije. Dobijeni rezultati dopunjuju naučnu literaturu koja se bavi ispitivanjem sličnih materijala i doprinose boljem razumevanju karakteristika dopiranih kiselina i njihovih bronzi različitim metalima.

Ključne reči: ciklična voltametrija, hronopotenciometrija, reakcije interkalacije/deinterkalacije litijuma, Li jonske baterije